Synthesis, cytotoxicity, apoptosis and cell cycle arrest of a ruthenium multi-substituted Keggin-type polyoxotungstate

Shifang Jia
Taiyuan University of Science and Tecnology
Yanzhen Wen
Taiyuan University of Science and Tecnology
Xiuli Hao
Taiyuan University of Science and Tecnology
Yan Zhang (yanzhang872010@163.com)
Taiyuan University of Science and Tecnology

Research Article

Keywords: Ruthenium multi-substituted polyoxometalate, Cytotoxicity, Cell apoptosis, Cell cycle arrest

Posted Date: September 7th, 2021

DOI: https://doi.org/10.21203/rs.3.rs-863084/v1

Abstract

The ruthenium multi-substituted polyoxotungstate with chemical formulae of $K_7[SiW_9O_{37}Ru_4(H_2O)_3Cl_3]\cdot 15H_2O$ (**S1**) was synthesized by a conventional aqueous solution containing the trilacunary Keggin-anions β-$Na_9HSiW_9O_{34}\cdot 12H_2O$(**S2**) and $RuCl_3\cdot nH_2O$(**S3**). Compound **S1** was characterized by elemental analyses, EDS, TG analyses, IR, UV/Vis and XPS. The cytotoxic potential of compound **S1** was tested on C33A, DLD-1, HepG-2 cancer cells and human normal embryonic lung fibroblasts cell MRC-5. The viability of the treated cells was evaluated by MTT assay. The mode of cell death was assessed by morphological study of DNA damage and apoptosis assays. Compound **S1** induced cell death in a dose-dependent manner, and the mode of cell death was essentially apoptosis though necrosis was also noticed. Cell cycle analysis by flow cytometry indicated that compound **S1** caused cell cycle arrest and accumulated cells in S phase.

1. Introduction

Cancer has become one of the serious public health problems which has threatened human health in the world. At present, chemotherapy has been an important means and approach for cancer treatment. Therefore, to find an effective and low-toxicity drug has become the priority in the chemotherapeutic treatment of tumors[1–3]. In clinical application and experimental exploration, most of the chemotherapeutic drugs mainly composed of synthetical compounds and adjuvant chemotherapeutic of natural substances or photochemicals. Among them, the synthetical compounds have many advantages, such as designability, controllability and predictability, which attractted wide attention from researchers. In recent years, it is worth noting that polyoxometalates (POMs) are intriguing biomedical agents due to their versatile bioactivity that endows antibacterial, antitumor, and antiviral functions[4–7]. Compared with current drugs, the unique advantage of POMs lies in the fact that the composition, molecular structure and physiochemical properties are adjustable and can be easily synthesized from readily available precursors in a few synthetic steps[8–11]. More importantly, another advantage of POMs is that transition metals can be introduced into their structure to obtain transition metal-substituted POMs, such as mono, dis or tri-substituted polyanions[12–14]. The combination of transition metals and vacancy POMs changed the composition, charge and physicochemical properties of the original saturated POMs, which also showed certain advantages in biological activity[15, 16].

In addition, ruthenium compounds, owing to the low energy barrier between their oxidation states, low atomic radius (0.125 nm) in transition metal series, and high solubility in water, which is conducive to accumulation in cancer tissues, have potential value in the development of chemotherapeutic drugs[17, 18]. Therefore, the synergistic effect of ruthenium and vacancy POMs is expected to endow ruthenium-substituted polyoxometalates (Ru-POMs) with high antitumor activity. At present, a multitude of Ru-POMs have been reported[19–27]. It is noteworthy that the antitumor activities of these compounds have been seldom reported. During our research on the exploration of Ru-POMs, the antitumor activities of a monoruthenium(II)-substituted Dawson polyoxotungstate have been investigated[28]. However, we also

noticed that the majority of the syntheses of Ru-POMs have used the monolacunary Keggin $[XW_{11}O_{39}]^{n-}$ (X = P, Ge and Si) or Dawson-type $[P_2W_{17}O_{61}]^{10-}$ polyoxoanions as reagents/ligands for the coordination to ruthenium[19–25]. The compounds synthesized by other types of lacancy POMs and ruthenium were rarely reported.

Based on aforementioned considerations, we choose trilacunary POMs β-$[SiW_9O_{34}]^{10-}$ (β-SiW_9) and $RuCl_3{\cdot}nH_2O$ as raw materials, preparing a ruthenium multi-substituted polyoxometalates, $K_7[SiW_9O_{37}Ru_4(H_2O)_3Cl_3]{\cdot}15H_2O$ (**S1**). Furthermore, the cytotoxicity of compound **S1** in vitro was evaluated by MTT (3-(4,5-dimethylthiazol-2-yl)-2,5-diphenyltetrazolium bromide) assay. The morphological apoptosis and the percentage of necrotic and apoptotic C33A (human cervical cancer) cells induced by the complex were also studied by fluorescence microscopy and flow cytometry. The cell cycle distribution of C33A cells was investigated by flow cytometry. The results indicated that compound **S1** could inhibit cell proliferation and induce apoptosis in cancer cells.

2. Experimental

2.1 Materials and instrumentation

All reagents and solvents were of commercial origin and were used without further purification unless otherwise noted. Ultrapure Milli-Q water was used in all experiments. β-$Na_9HSiW_9O_{34}{\cdot}12H_2O$ was prepared according to the reported methods.[29] RPMI 1640 was purchased from Sigma. C33A (human cervical cancer), DLD-1 (human colon cancer), HepG-2 (human liver cancer), MRC-5 (human normal embryonic lung fibroblasts) cell lines were purchased from the American Type Culture Collection. W, Ru and K were determined by a Leaman inductively coupled plasma (ICP) spectrometer. Cl was analyzed by ion chromatography. Energy-dispersive X-ray spectroscopy (EDS) was performed by X-Max Extreme. TG analyse was carried out on a Pyris Diamond TG instrument in flowing N_2 with a heating rate of $10°C{\cdot}min^{-1}$. Infrared spectra was recorded on a Perkin-Elmer Spectrum FT-IR Spectrometer using KBr pellets. Raman spectrum was tested by the Raman spectrometer. Electronic absorption spectra (UV/Vis) was recorded on a Lambda750 spectrophotometer. X-ray photoelectron spectroscopy (XPS) of Ru and W were measured on a VG ESCALAB MK II spectrometer with a Mg Kα (1253.6 eV) achromatic X-ray source. Solution electronic emission spectra in acetonitrile was recorded on Shimadzu 3100 spectrophotometer and Shimadzu RF-5301 PC spectrofluorometer. Cyclic voltammetry (CV) was obtained with CHI 630E instrument in a three-electrode cell: glassy carbon electrode (GCE, diameter 3 mm) as a working electrode, platinum wire as a counter electrode, and Ag/AgCl as a reference electrode.

2.2 Synthesis

$K_7[SiW_9O_{37}Ru_4(H_2O)_3Cl_3]{\cdot}15H_2O$ (**S1**)

About 0.27 g of $RuCl_3{\cdot}nH_2O$ (1.1 mmol) was dissolved in 8 ml of water, and 1.00 g (0.37 mmol) of solid β-$Na_9HSiW_9O_{34}{\cdot}12H_2O$ was added very slowly, with vigorous stirring at room temperature (addition should

last about 1h). The pH was then adjusted to 5.5 with aqueous Na_2CO_3 (1 M), the resulting solution heated to 70–80 ℃ and stirred at this temperature for half an hour. After cooling, aqueous Na_2CO_3 was again added to adjust the pH 5.0, and the solution filtered to remove any solid impurities. The aqueous solution obtained was passed three times through an Amberlite cationic column (IR-120) in the K^+ form. KCl (1.0 g, 13 mmol) was then added the resulting solution with stirring and black solids were precipitated immediately. The black solids were filtered after 24 h. Anal. Calc.: W, 48.94; Ru, 11.94; K, 8.07; Cl, 3.15. Found: W, 49.75; Ru, 12.25; K, 8.19; Cl, 3.09. Molar ratio W/ Ru = 2.23.

2.3 Methods

2.3.1 Cytotoxicity assay in vitro

Standard MTT assay procedures were used[30]. Cells were placed in 96-well microassay culture plates (8×10^3 cells per well) and grown overnight at 37°C in a 5% CO_2 incubator. The complex tested was then added to the wells to achieve final concentrations ranging from 2.5 to 100 μM. Control wells were prepared by addition of culture medium (200 μL). The plates were incubated at 37°C in a 5% CO_2 incubator for 24□48 or 72 h. On completion of the incubation, stock MTT dye solution (20 μL, 5 mg/mL) was added to each well. After 4 h, 150 mL dimethylsulfoxide (DMSO) was added to solubilize the MTT formazan. The optical density of each well was then measured with a microplate spectrophotometer at a wavelength of 490 nm. The IC_{50} values were determined by plotting the percentage viability versus the concentration and reading off the concentration at which 50 % of the cells remained viable relative to the control. Each experiment was repeated at least three times to obtain the mean values. Three different tumor cell lines were the subjects of this study: C33A, DLD-1 and HepG-2. And MRC-5 is the normal cell. These cells were purchased from the American Type Culture Collection (Rockville, MD, USA).

2.3.2 Apoptosis assay by Hoechst 33342 staining

C33A cells were seeded onto chamber slides in six-well plates at a density of 2×10^5 cells per well and incubated for 24 h. The cells were cultured in RPMI 1640 supplemented with 10 % fetal bovine serum (FBS) and incubated at 37°C and 5 % CO_2. The medium was removed and replaced with medium (final DMSO concentration, 0.05 % v/v) containing the complex for 48 h. The medium was removed, and the cells were washed with ice-cold phosphate-buffered saline(PBS), and fixed with formalin (4%, w/v). Cell nucleus were counterstained with Hoechst 33342 (10 mg/mL in PBS) for 10 min. Then the cells were observed and imaged by a fluorescence microscope (Nikon, Yokohama, Japan) with excitation at 350 nm and emission at 460 nm.

2.3.3 Apoptosis assay by flow cytometry

After chemical treatment, 2×10^5 cells were harvested, washed with PBS, then fixed with 70% ethanol, and finally, maintained at 4°C for at least 12 h. Then the pellets were stained with the fluorescent probe solution containing 50 μg/mL propidium iodide and 1 mg/mL Annexin in PBS on ice in the dark for 15

min. The fluorescence was then measured at 530 and 575 nm using 488-nm excitation by a FACS Calibur flow cytometry system. A minimum of 10,000 cells were analyzed per sample.

2.3.4 Cell cycle arrest investigated by flow cytometry

C33A cells were seeded into six-well plates at a density of 2×10^5 cells per well and incubated for 24 h. The cells were cultured in RPMI 1640 supplemented with FBS (10%) and were incubated at 37°C and 5% CO_2. The medium was removed and replaced with medium (final DMSO concentration, 0.05 % v/v) containing complex. After incubation for 24 h, the cell layer was trypsinized and washed with cold PBS and fixed with 70 % ethanol. 20 µL of RNase (0.2 mg/mL) and 20 µL of propidium iodide (0.02 mg/mL) were added to the cell suspensions and they were incubated at 37°C for 30 min. Then the samples were analyzed with a FACS Calibur flow cytometry system. The number of cells analyzed for each sample was 10,000.

3. Results And Discussion

3.1 Synthesis and characterization

Compound **S1** was obtained from solutions that were passed several times through an Amberlite cationic column in the potassium form, in order to eliminate the possibility of excessive non-coordinated Ru. This seems to indicate that Ru does not coprecipitate as counter-cation of the potassium salts of the polyoxoanions, but is included in the new formed complexes with the trilacunary species. In other words, this suggests that four ruthenium atoms must be coordinated to one SiW_9 anion. According to the results of elemental analysis, the ratio of W/Ru in the compound **S1** is 2.23, which proves the presence of four Ru atoms per SiW_9 unit. Additionally, three chloride ions per SiW_9 were found by analysis of ion chromatography. The existence of W, Ru, K, Cl, O was further confirmed by EDS (Fig. 1). The TG curve of compound **S1** (Fig. 2) displays the weight loss of 9.66% in the temperature range of 30 ~ 325°C, corresponding to three coordinated water molecules and fifteen lattice water molecules (calculated value 9.58%). Based on analytical results and charge balance considerations, the molecular formula of compound **S1** can be determined as $K_7[SiW_9O_{37}Ru_4(H_2O)_3Cl_3]\cdot15H_2O$[31], which possibly possess construction being similar to that already observed for the Ni substituted polyoxometalate, $[PW_9O_{34}Ni^{II}_3(OH)_3(H_2O)_3Ni(H_2O)_3]^{4-}$ (PW_9Ni_4) [32] (Fig. 3).

The IR spectrum of compound **S1** are shown in Fig. 4. In the spectrum, characteristic bands at 1002 cm^{-1}, 955 cm^{-1}, 895 cm^{-1}, and 782 cm^{-1} are attributed to v(Si-O), v(W-O_d) and v(W-$O_{b/c}$-W), respectively[31]. The Raman spectrum of compound **S1** showed fewer split bands: W-O_d (953 cm^{-1}), W-O_b-W (898 cm^{-1}) and W-O_c-W (778 cm^{-1}) (Fig. 5). The consistency between Raman and IR spectrum confirmed the stability of the compound **S1** in aqueous solution.

Electronic absorption spectra (UV/Vis) of compound **S1** in aqueous solution showed a band of high intensity in the visible region, centred at about 435nm (Fig. 6), as observed for other Ru^{III}

polyoxoanions[33–36]. X-ray photoelectron spectroscopy (XPS) was used to identify the W/Ru oxidation states. XPS spectra of W 4f in compound **S1** shows two partially overlapped peaks which at 35.18 and 37.38 eV are assigned to $4f^{7/2}$ and $4f^{5/2}$ of W(VI) center (Fig. 7a)[37]. The binding energy peaks at 282.38 and 286.48 eV corresponds to $3d^{5/2}$ and $3d^{3/2}$ of the Ru(III) center (Fig. 7b)[31].

3.2 Luminescence spectra studies

The solid-state fluorescent of **S1** was studied by fluorescence spectrum. Compound **S1** upon excitation onto their excitation maxima exhibited an emission band at 590 nm. The emission profile and emission maxima was similar and independent of the excitation wavelength. The electronic emission spectral of compound **S1** was presented in Fig. 8a. Moreover, solution-state fluorescent of compound **S1** was also studied, the complex exhibited an emission band at 685 nm (Fig. 8b).

3.3 Cyclic voltammetry

The redox behavior of compound **S1** has been investigated in Na_2SO_4 (0.5 M)/H_2SO_4 (1M) solution with pH = 3 to complement the spectroscopic data. The investigation of electrochemical behavior was very useful to determine the extent of electronic interaction between the metal centers. The cyclic voltammogram of $RuCl_3{\cdot}nH_2O$ showed no redox peak in the range of -0.5 to 1.0 V. The cyclic voltammetry (CV) measurements of compound **S1** with the scan rate of 50 mV/s were recorded in the potential range from + 1000 to -700 mV in sulfate buffers with pH = 3 (Fig. 9). As shown in Fig. 9, the mean peak potentials ($E_{1/2}=(E_{cp} + E_{ap})/2$) for I-I' of reversible redox peaks are 300 mV, which was assignable to the $Ru^{III/II}$ couple[38].

3.4 Cytotoxicity assay in vitro

The cytotoxicity of the **S1, S2** and **S3** was studied in C33A, DLD-1, HepG-2 and MRC-5 cell lines by means of the MTT cell survival assay. C33A, DLD-1, HepG-2 and MRC-5 cells were treated with different concentrations of complexes **S1-3** for 24、48 and 72h. For 24 h (Fig. 10a), the complexes showed the weak activity to the three cell lines with IC_{50} values were 74.06 μM for C33A, 89.05 μM for DLD-1 and more than 100μM for HepG2 of **S1**. The IC_{50} values of **S2** and **S3** to three cell lines were more than 100μM. For 48 h (Fig. 10b), the **S1** showed the weak activity in the C33A and DLD-1 with IC_{50} values of 75.72 and 89.73μM, respectively, and IC_{50} values of more than 100μM for HepG2. However, **S2** and **S3** showed the weak activity to the three cell lines with IC_{50} values were nearly 100 μM. For 72 h (Fig. 10c), the IC_{50} of the **S1** was 45.48μM for C33A, 78.32μM for DLD-1 and 95.08μM for HepG-2. It is worth noting that the complexes have no cytotoxicity to the normal cell MRC-5 in different time, the IC_{50} values were more than 100 μM. The IC_{50} of **S1-3** to C33A, DLD-1 and HepG-2 in different time were displayed in Table

1. Cytotoxicity of some Keggin and lacunary-Keggin sandwiched polyoxotungstates towards Madin-Darby canine kidney (MDCK), Vero, HEp-2, and MT-4 cells was investigated by using MTT. All the compounds did not show any toxicity at concentrations of < 200 μM for MDCK, Vero, and HEp-2 cells[39]. All of these comparisons led to the conclusion that the complexes we studied had greater antitumor activity than reported. Obviously, the cell viability was found to be concentration-dependent and duration-dependent, which indicated that the **S1** entered the cells slowly and killed the cells gradually. During three cell lines, **S1** showed the highest activity to C33A, secondly DLD-1, finally HepG2.

Table 1
IC_{50} values of complexes against human tumor cell lines

Time	Complexes	IC_{50}(μM)		
		C33A	DLD-1	HepG-2
24h	**S1**	74.06 ± 1.32	89.05 ± 1.75	> 100
	S2	> 100	95.08 ± 2.72	> 100
	S3	> 100	> 100	> 100
48h	**S1**	75.72 ± 2.52	89.73 ± 0.42	> 100
	S2	91.25 ± 0.98	> 100	> 100
	S3	90.42 ± 1.53	89.59 ± 1.93	> 100
72h	**S1**	45.48 ± 1.22	78.32 ± 1.48	95.08 ± 1.66
	S2	87.25 ± 0.35	90.51 ± 0.37	> 100
	S3	85.47 ± 1.76	80.12 ± 2.62	> 100

3.5 Apoptosis studies by Hoechst 33342 staining and flow cytometry

Hoechst 33342, which stains the cell nucleus, is a membrane permeable dye with blue fluorescence. Live cells with uniformly light blue nuclei were observed under fluorescence microscope after treatment with Hoechst 33342, while apoptotic cells had bright blue nuclei on account of karyopyknosis and chromatin condensation, whereas, the nuclei of dead cells could not be stained[40]. C33A cells dealt with **S1** at 5□25 and 50 μM for 48 h were stained with Hoechst 33342. C33A cells without dealing with the **S1** was used as control. The results were given in Fig. 11. In the control, cells show homogeneous nuclear staining. After treatment of C33A cells with **S1**, the number of apoptotic cells increases in a dose-dependent manner and they exhibit typical apoptotic features, such as staining brightly, condensed chromatin, and fragmented nuclei. These results show the **S1** can effectively induce the apoptosis against C33A cells.

The morphological apoptosis studies showed **S1** can induce apoptosis of C33A cells. To determine the percentages of apoptotic and necrotic cells, C33A cells without dealing with the **S1** was used as control, apoptosis was investigated by flow cytometry, as shown in Fig. 12 In the control, the proportions of living cells and apoptotic cells were 99.6 and 0.3 %, respectively. After C33A cells have been exposed to **S1** (5、25、50 μM) for 48 h, the proportions of apoptotic cells were 3.6, 11.6 and 54.5 %, respectively. Comparing with the control, the proportion of living cells decreased and apoptotic cells increased. These data demonstrate that the apoptotic effect on C33A cells for **S1** is concentration-dependent, with increasing concentrations of **S1**, the number of apoptotic cells increases.

3.6 Cell cycle arrest

The distribution of C33A cells in various compartments during the cell cycle was analyzed by flow cytometry in cells stained with propidium iodide. As shown in Fig. 13, treatment of C33A cells with 5、25、50 μM **S1** for 48 h cause significant enhancement of 2.5, 7.9 and 16.5 % in S phase compared with the control, treatment of C33A cells with 50 μM **S1** for 48 h cause decrease of 20.5 in G_0/G_1 phase compared with the control. These data show that **S1** induce S-phase arrest in C33A cells[41].

4. Conclusions

In summary, the introduction of ruthenium into the trilacunary POMs reaction system obtains a ruthenium multi-substituted polyoxometalates. In vitro, compound **S1** exhibits higher cytotoxicity toward C33A than DLD-1 and HepG-2 cell lines under identical conditions. Hoechst 33342 staining demonstrated that compound **S1** can effectively induce apoptosis of C33A cells. Apoptosis assay by flow cytometry showed the number of apoptotic cells increased with increasing concentration of compound **S1**. The cell cycle arrest studies demonstrated that the antiproliferative effect induced by compound **S1** on C33A cells occurs in S phase. Thus, ruthenium-substituted polyoxometalates can be used as new potential candidate for chemotherapy drugs in the field of tumor chemotherapy. However, the possible mechanism of compound **S1** on apoptotic induction in cancer cells needs to be further studied. This work is ongoing in our group.

Declarations

Acknowledgements

This work was supported by the National Natural Science Foundation of China (No. 21701120) and the Science and Technology Innovation Project of Colleges and Universities in Shanxi Province (No. 2020L0334).

Competing interests: The authors declare no competing interests.

References

1. Huang X, Zhang Z, Jia L, Zhao Y, Zhang X, Wu K. *Cancer. Lett.*, 2010,**296**:123–131
2. Liu H K, Wang Q, Li Y, Sun W G, Liu J R, Yang Y M, Xu W L, Sun X R, Chen B Q. J. *Nutr. Biochem.*, 2010,**21**:206–213
3. Ghobrial I M, Witzig T E, Adjei A A. *CA Cancer J. Clin.*, 2005,**55**:178–194
4. Hasenknopf B. *Front. Biosci. Landmark Ed.*, 2005,**10**:275–287
5. Li H, Gong H W, Qi Y F, Li J, Ji X F, Sun J H, Tian R, Bao H, Song X F, Chen Q, Liu G L. *Scientific Reports.*, 2017,**7**:16942–16950
6. Gerth H U V, Rompel A, Krebs B, Boos J, Lanvers-Kaminsky C. *Anti-Cancer Drugs.*, 2005,**16**:101–106
7. Wang J, Liu Y, Xu K, Qi Y F, Zhong J, Zhang K, Li J, Wang E B, Wu Z Y, Kang Z H. *Appl. Mater. Interfaces.*, 2014,**6**:9785–9789
8. Herve M, Sinoussi-Barre F, Chermann J, Hervé G, Jasmin C. *Biochem. Biophys. Res. Commun.*, 1983,**116**:222–229
9. Aureliano M, Gândara R M, *J. Inorg. Biochem.*, 2005,**99**:979–985
10. Lee I S, Long J R, Prusiner S B, Safar J G, *J. Am. Chem. Soc.*, 2005,**127**:13802–13803
11. Müller C E, Iqbal J, Baqi Y, Zimmermann H, Röllich A, Stephan H. *Bioorg. Med. Chem. Lett.*, 2006,**16**:5943–5947
12. Balula, S S, Santos I C M S, Barbosa A D S, Schlindwein W, Cavaleiro A M V, De Castro B, Cunha-Silva L. *Materials Science Forum.*, 2013,**730**:975–980
13. Kikukawa Y, Suzuki K, Yamaguchi K, Mizuno N. *Inorg. Chem.*, 2013,**52**:8644–8652
14. Dutta D, Jana A D, Debnath M, Mostafa G, Clérac R, Tojal J G, Ali M. *Eur. J. Inorg. Chem.*, 2010,5517–5522
15. Wang L, Zhou B B, Yu K, Su Z H, Gao S, Chu L L, Liu J R, Yang G Y. *Inorg. Chem.*, 2013,52:5119–5127
16. Wang L, Yu K, Zhou B B, Su Z H, Gao S, Chu L L, Liu J R. *Dalton Trans.*, 2014,**43**:6070–6078
17. Sava G, Bergamo A, *Int. J. Oncol.*, 2000,**17**:353–365
18. Rademaker-Lakhai J M, van den Bongard D, Pluim D, Beijnen J H, Schellens J H. *Clinical cancer research: an official journal of the American Association for Cancer Research*, 2004,**10**:3717–3727
19. Sadakane M, Tsukuma D, Dickman M H, Bassil B S, Kortz U, Capron M, Ueda W. *Dalton Trans.*, 2007,2833–2838
20. Yokoyama A, Ohkubo K, Ishizuka T, Kojima T, Fukuzumi S. *Dalton Trans.*, 2012,**41**:10006–10013
21. Lahootun V, Besson C, Villanneau R, Villain F, Chamoreau L, Boubekeur K, Blanchard S, Thouvenot R, Proust A. *J. Am. Chem Soc.*, 2007,**129**:7127–7135
22. Liu B, Yan J, Wang Y F, Yi X Y. *Dalton Trans.*, 2015,**44**:16882–16887

23. Liu H, Yue B, Sun W, Chen Z, Jin S, Deng J, Xie G, Shao Q, Wu T. *Trans. Met. Chem.*, 1997,**22**:321–325
24. Nomiya K, Torii H, Nomura K, Sato Y. *J. Chem. Soc. Dalton Trans.*, 2001,1506–1512
25. Ogo S, Shimizu N, Ozeki T, Kobayashi Y, Ide Y, SanoT J, Sadakane M. *Dalton Trans.*, 2013,**42**:2540–2545
26. Howells A R, Sankarraj A, Shannon C. *J. Am. Chem. Soc.*, 2004,**126**:12258–12259
27. Morris A M, Anderson O P, Finke R G. *Inorg. Chem.*, **2009,48**: 4411–4420
28. Jia S F, Hao X L, Wen Y Z, Zhang Y. *Journal of Coordinationg Chemistry.*, 2019,**72**:633–644
29. Tézé A, Hervé G. *Inorg. Synth.*, **1990**,**27**:88
30. T. Mosmann, *J. Immunol. Med.*, 1983,**65**:55–63
31. Gamelas J A F, Carapuca H M, Balula M S, Evtuguin D V, Schlindwein W, Figueiras F G, Amaral V S, Cavaleiro A M V. *Polyhedron*, 2010,**29**:3066–3073
32. Kortz U, Tézé A, Hervé G. *Inorg. Chem.*, 1999,**38**:2038–2042
33. Neumann R, Abu-Gnim C. *J. Am. Chem. Soc.*, 1990,**112**:6025–6031
34. Sadakane M, Higashijim M. *Dalton Trans.*, 2003,659–664
35. Neumann R, Khenkin A M, Dahan M. *Angew. Chem., Int. Ed.*, 1995,**34**:1587–1589
36. Quinonero D, Wang Y, Morokuma K, Khavrutskii L A, Botar B, Geletii Y V, Hill C L, Musaev D G. J. *Phys. Chem. B.*, 2006,**110**:170–173
37. Hao X L, Ma Y Y, Wang Y H, Xu L Y, Liu F C, Zhang M M, Li Y G. *Chem. Asian J.*, 2014,**9**:819–829
38. Landsmann S, Wessig M, Schmid M, Cölfen H, and Polarz S. *Angew. Chem. Int. Ed.*, 2012,**51**:5995–5999
39. Yamase T. *J. Mater. Chem.*, 2005,**15**:4773–4782
40. Li J F, Huang R Z, Yao G Y, Ye M Y, Wang H S, Pan Y M, Xiao J T. *Eur. J. Med. Chem.*, 2014,**86**:175–188
41. Zhang Y, Hu P C, Cai P, Yang F, Cheng G. Z. *RSC Adv.*, 2015,**5**:11591–11598

Figures

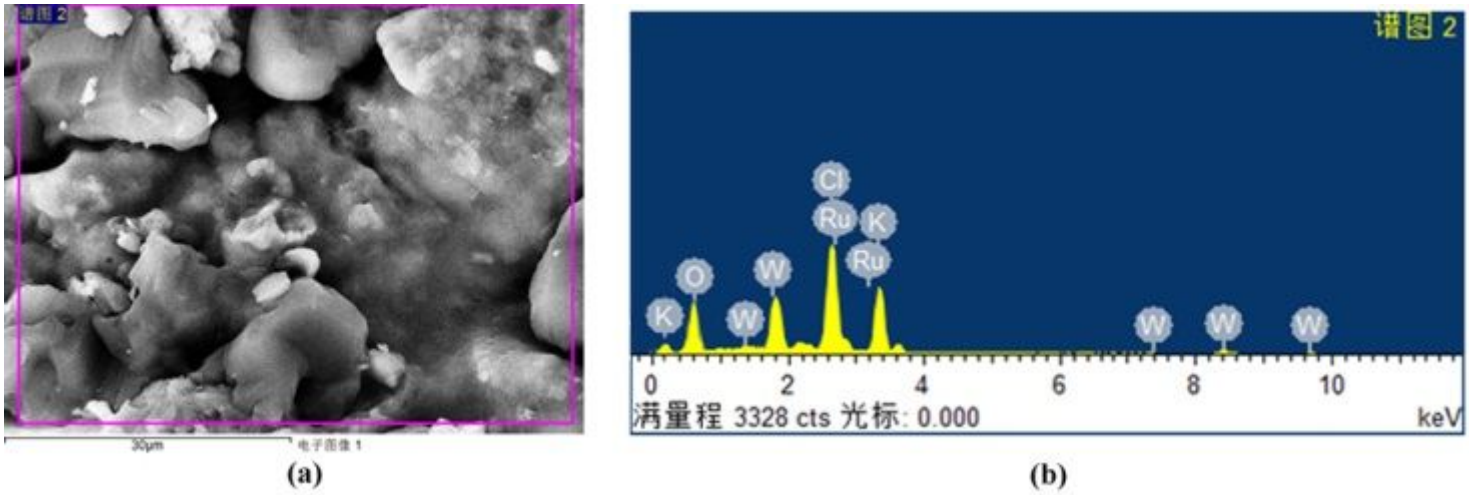

Figure 1

(a) SEM image of compound S1; (b) EDS of compound S1

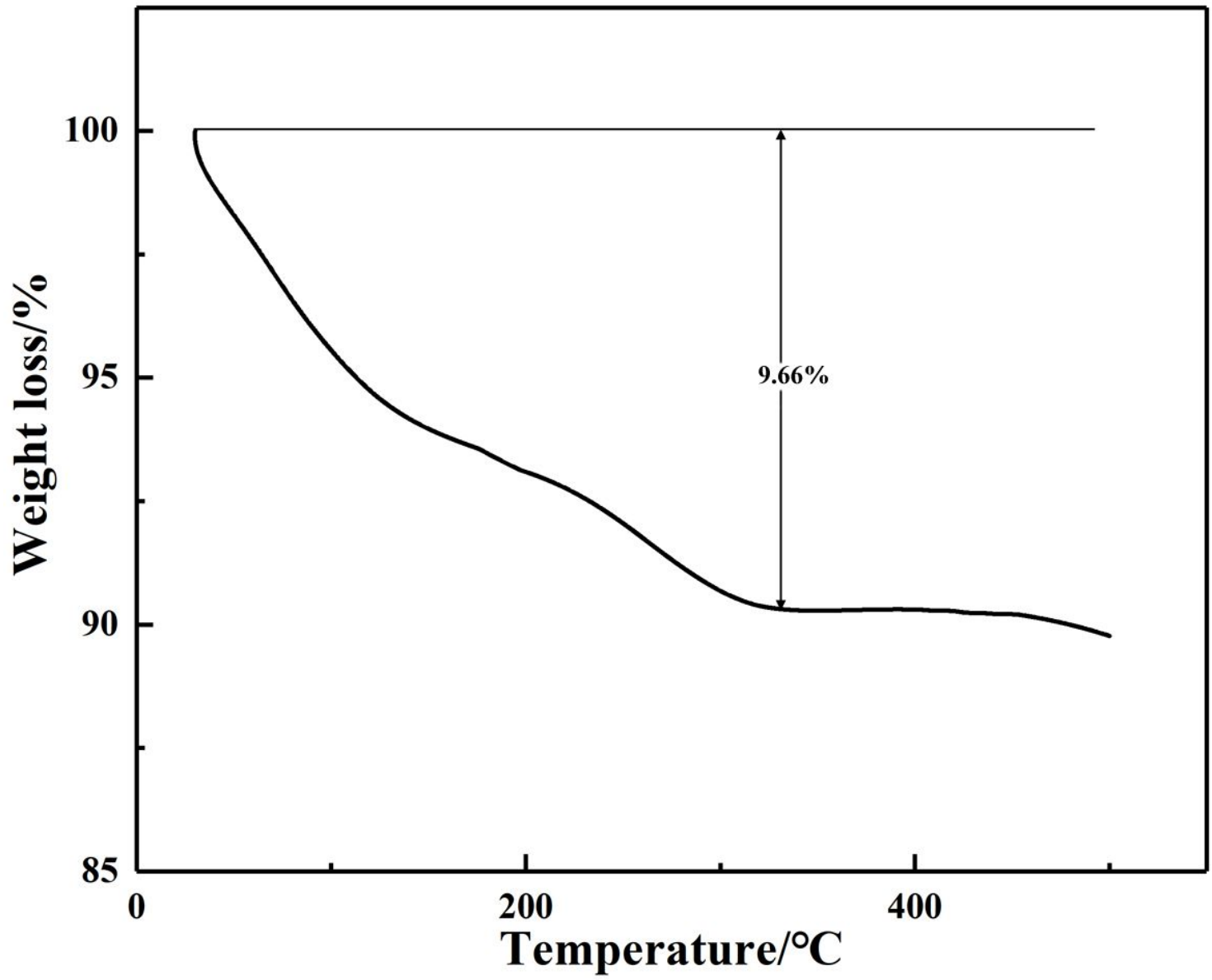

Figure 2

TG curve of compound S1

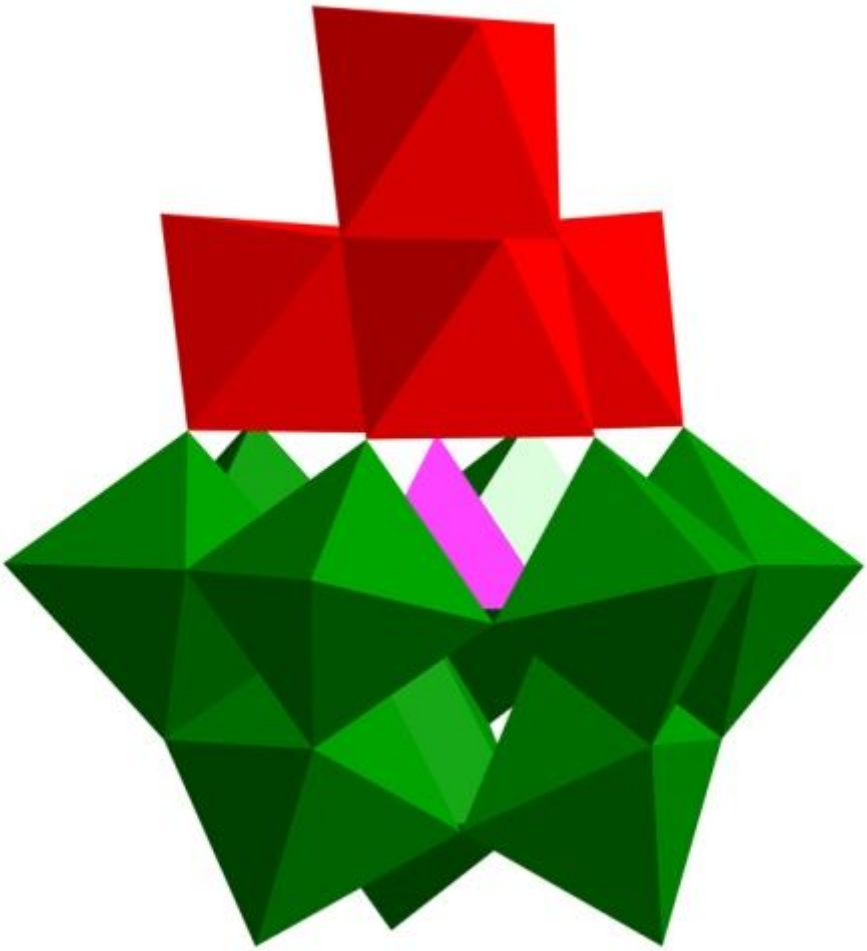

Figure 3

Possible structure for the Ru tetra-substituted anions [SiW9O37Ru4(H2O)3Cl3]7- in compounds S1

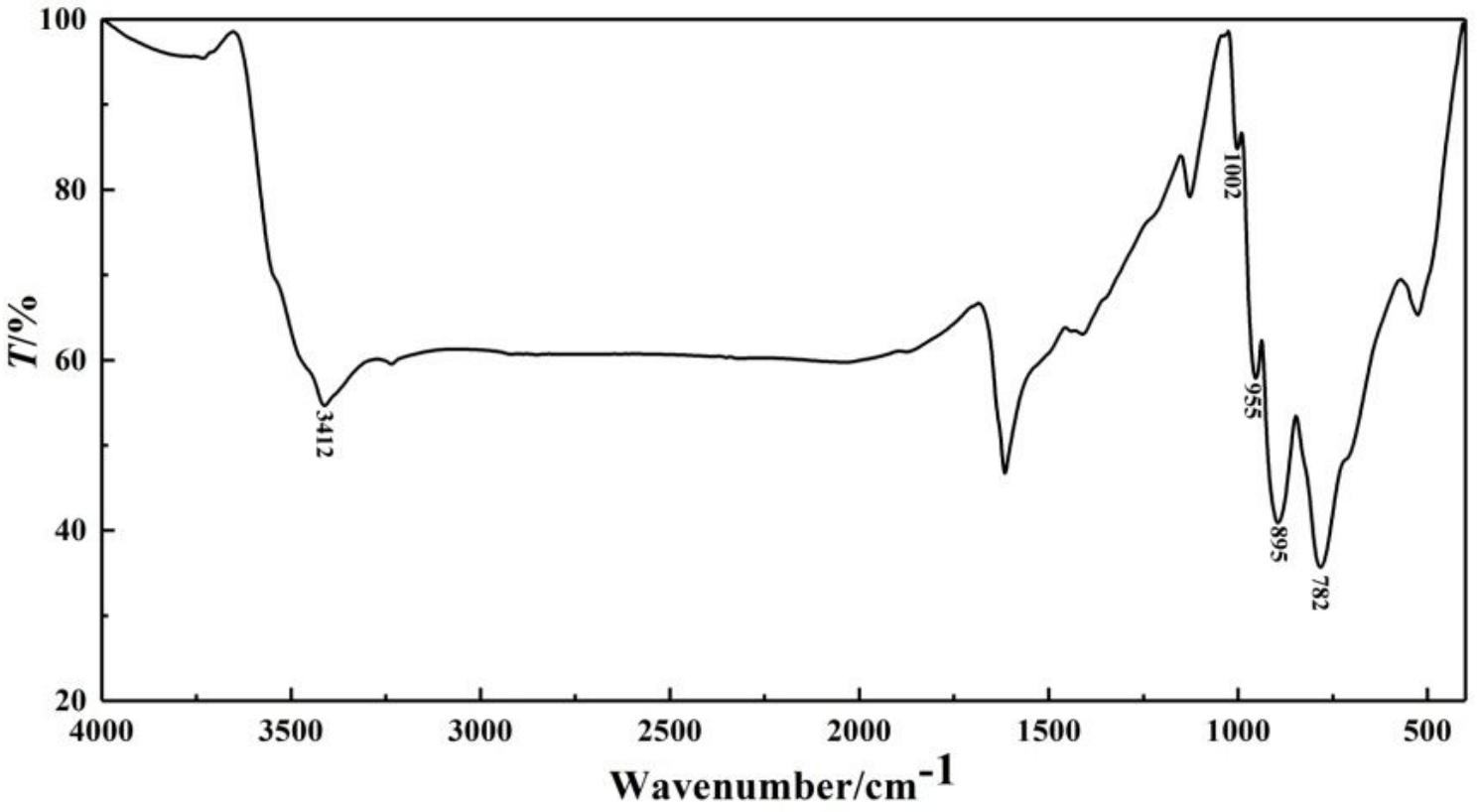

Figure 4

IR spectrum of compound S1

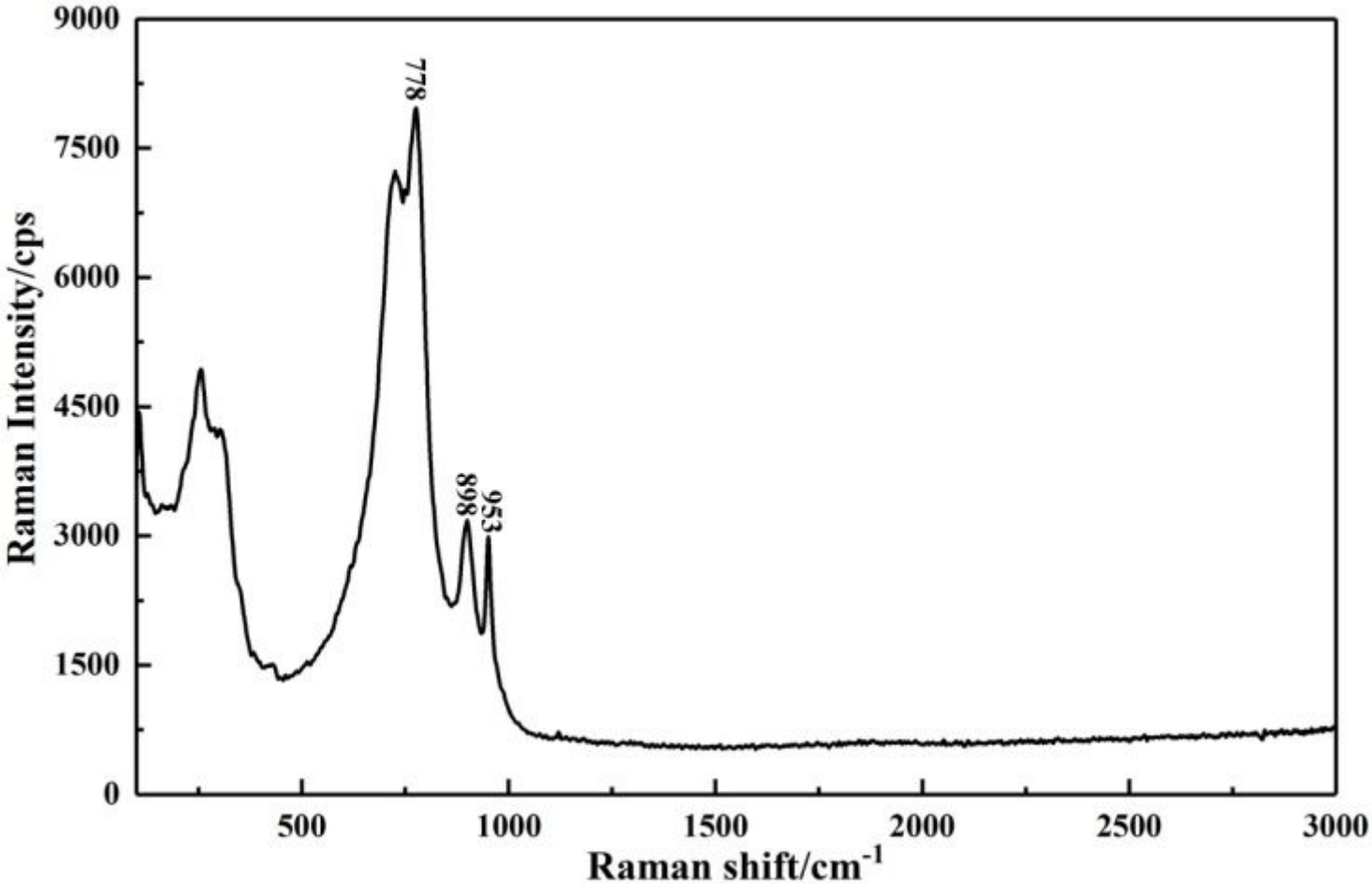

Figure 5

Raman spectrum of compound S1

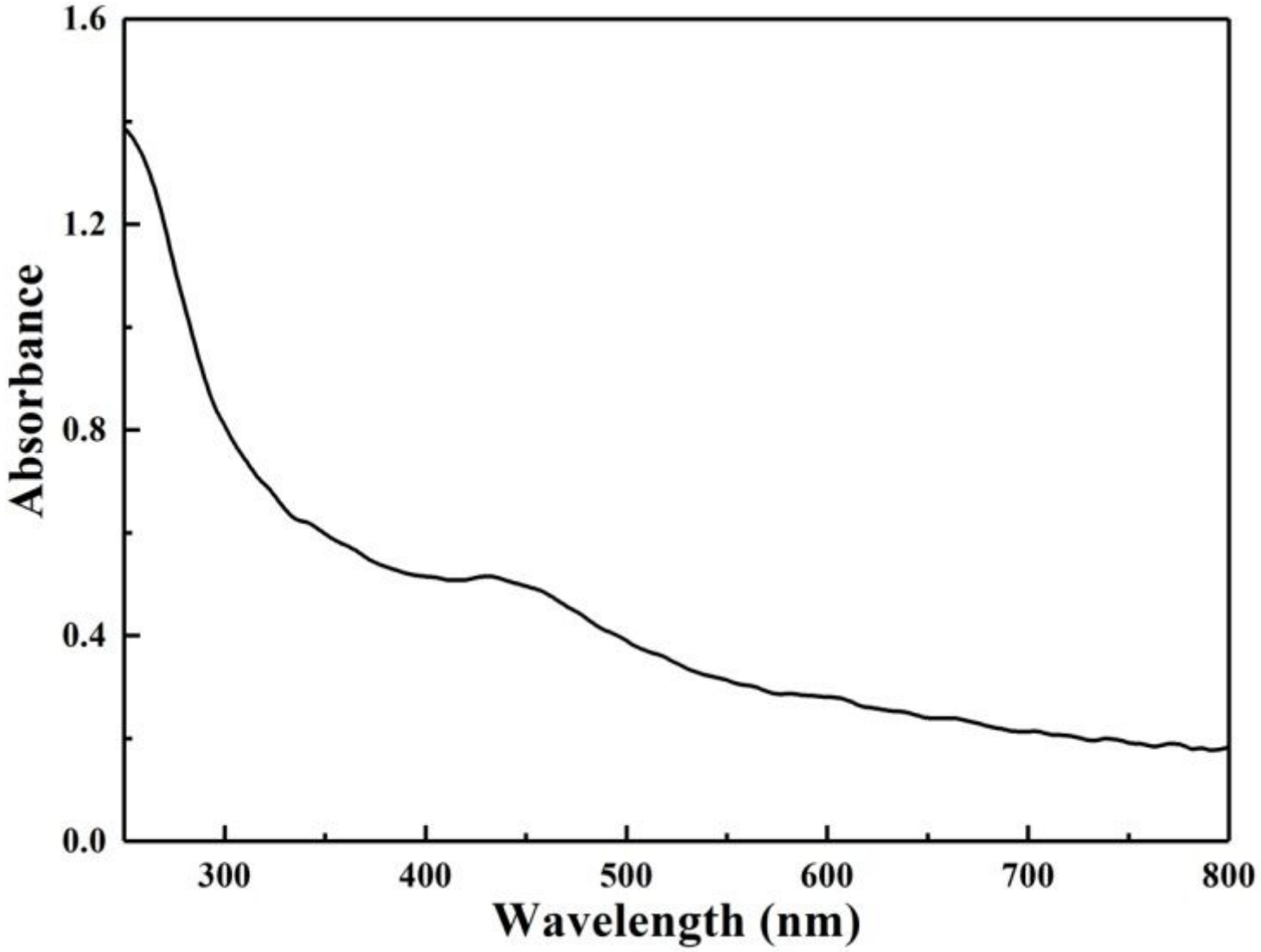

Figure 6

UV/Vis absorption spectrum of aqueous solution of compound S1

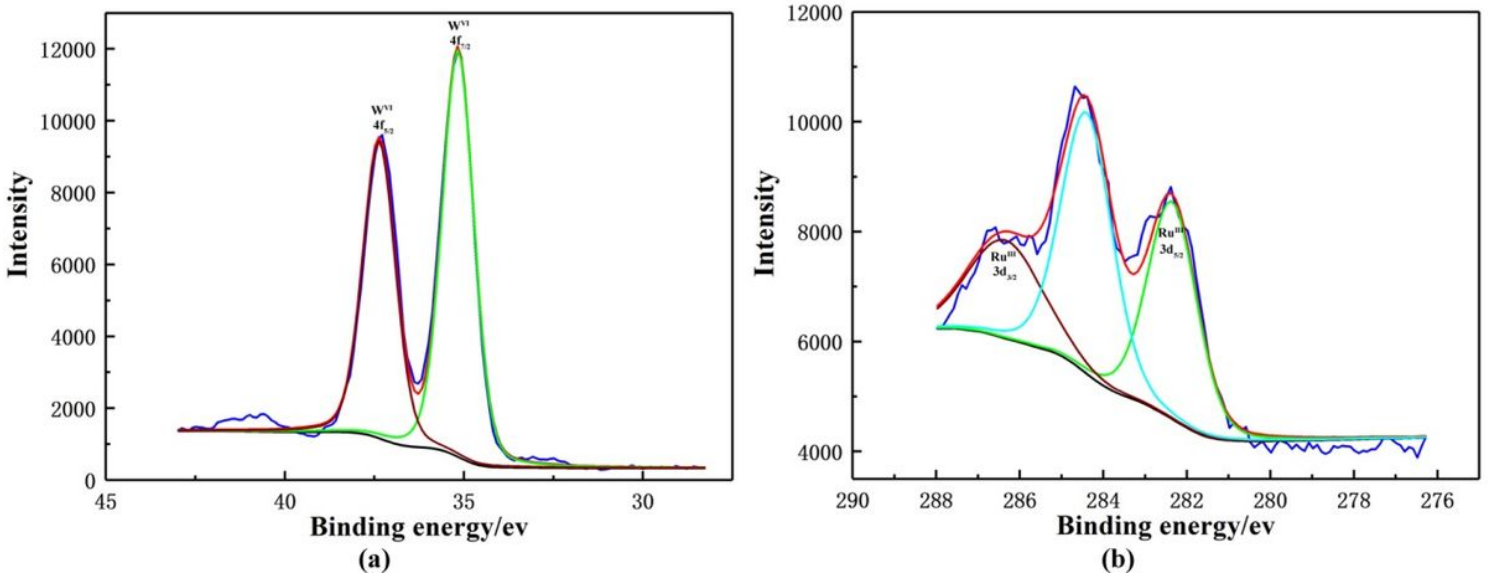

Figure 7

The XPS spectra of (a) W4f and (b) Ru3d in compound S1

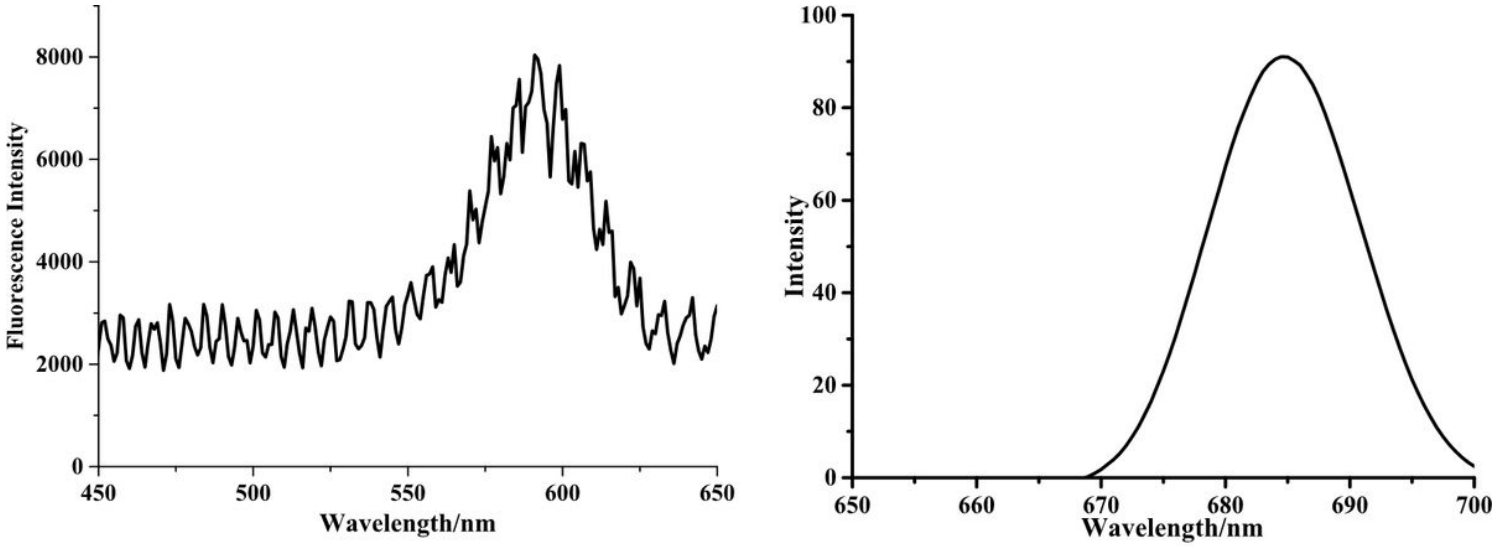

Figure 8

The fluorescence emission spectrum of the S1 (a) solid; (b) solution

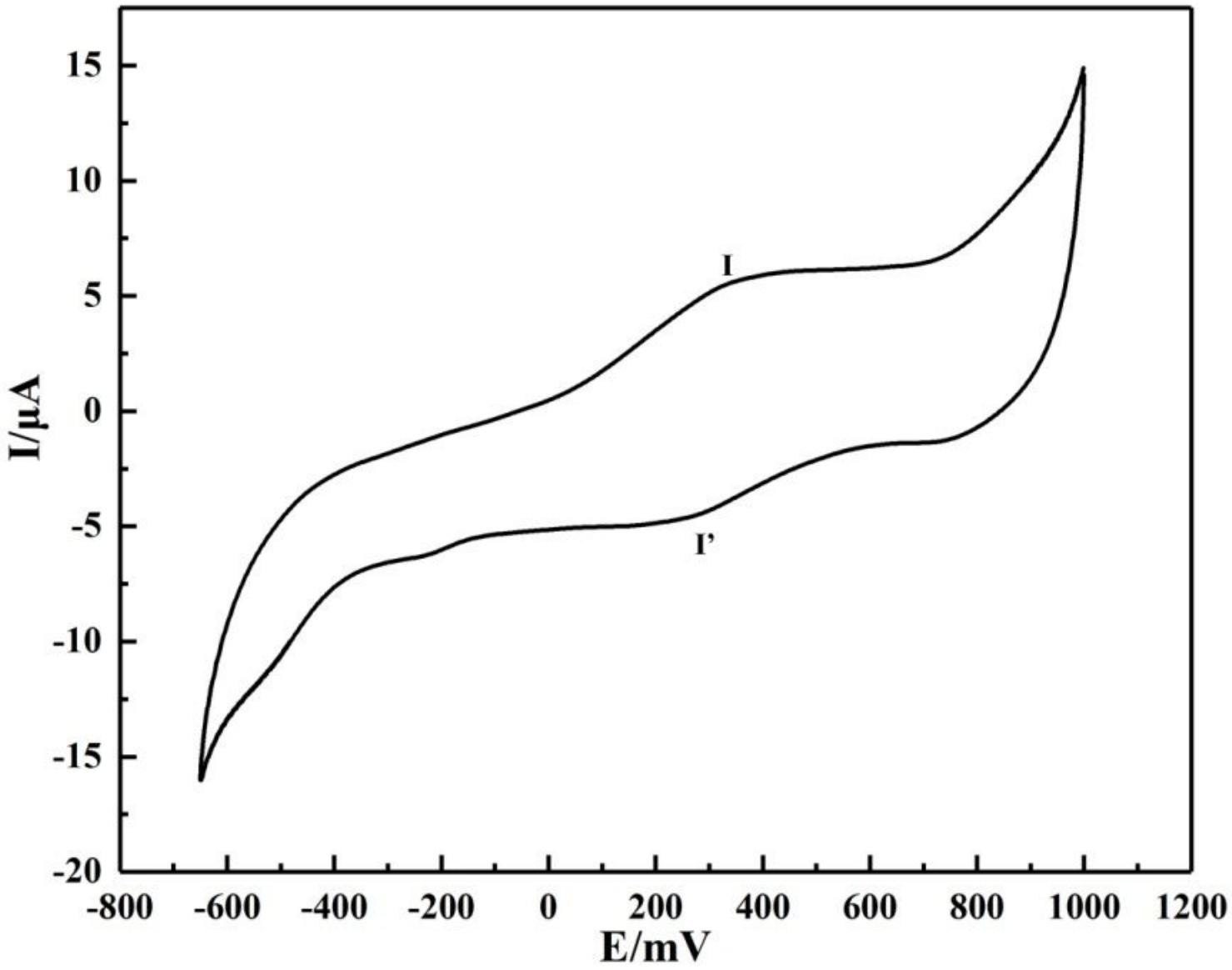

Figure 9

Cyclic voltammograms (scan rate 50 mV/s) of complex S1 for pH 3 in sulfate buffers.

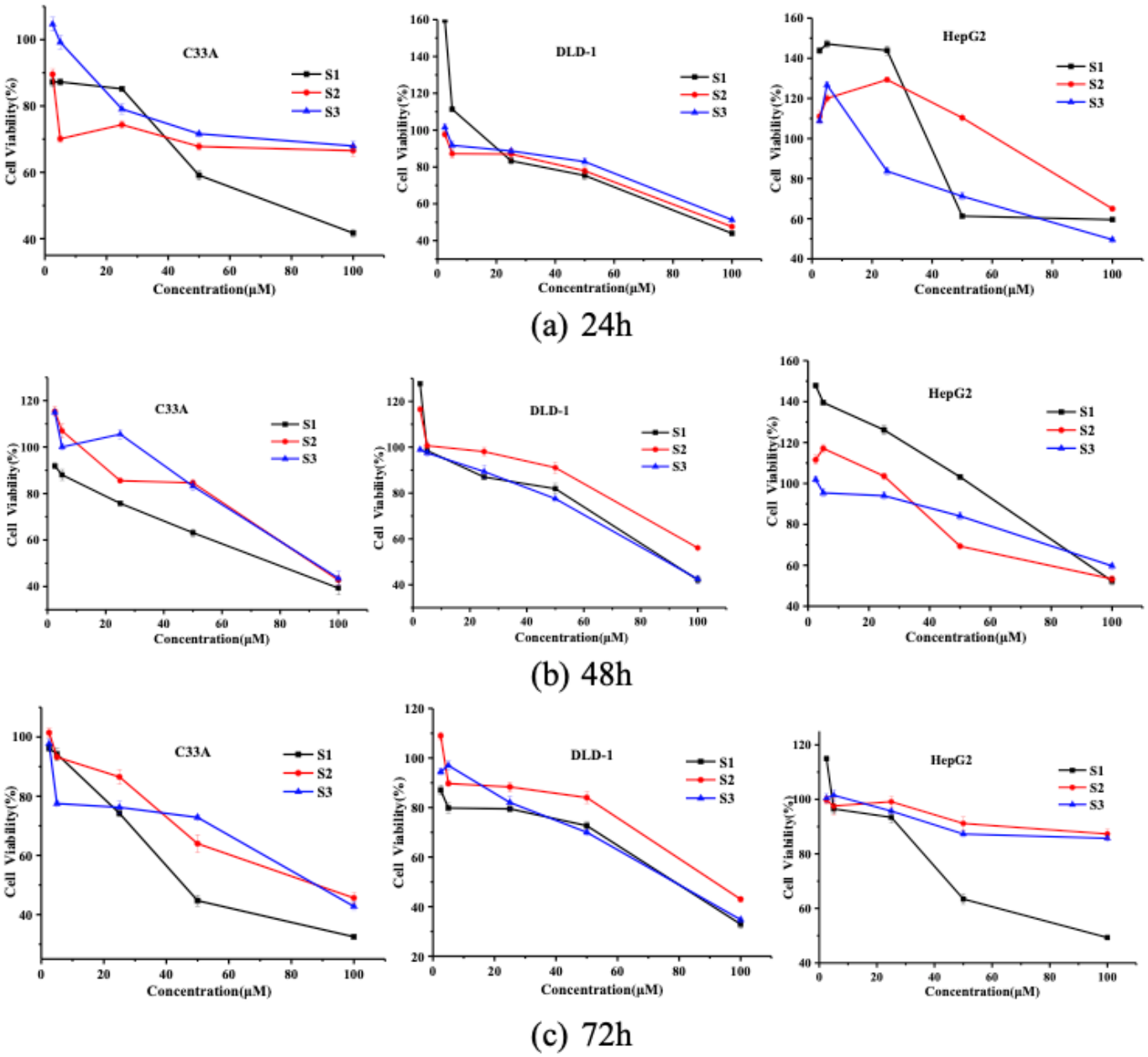

Figure 10

Cell viability inhibition induced by S1-S3. (a) C33A, DLD-1 and HepG-2 cells were treated with S1, S2 and S3 for 24 h. (b) C33A, DLD-1 and HepG-2 cells were treated with S1, S2 and S3 for 48 h. (c) C33A, DLD-1 and HepG-2 cells were treated with S1, S2 and S3 for 72 h. Cell viability was measured with the MTT assay. Data from three independent experiments run in triplicate cells were shown.

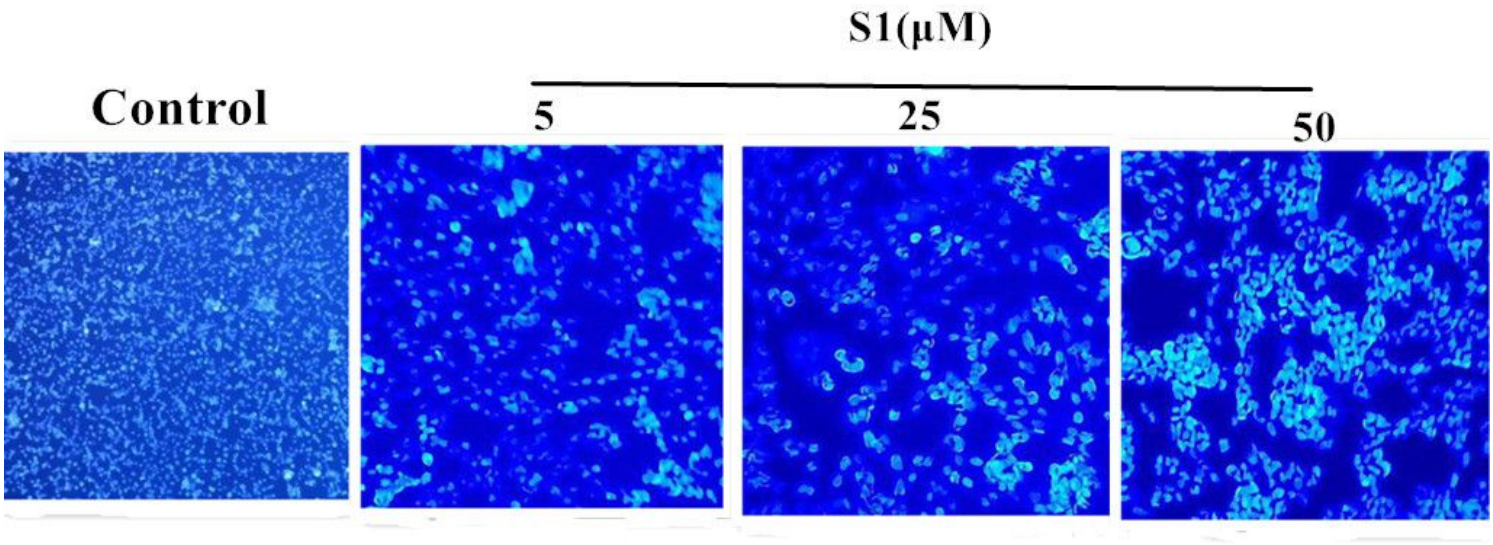

Figure 11

Hoechst 33342 staining of C33A cells 48 h

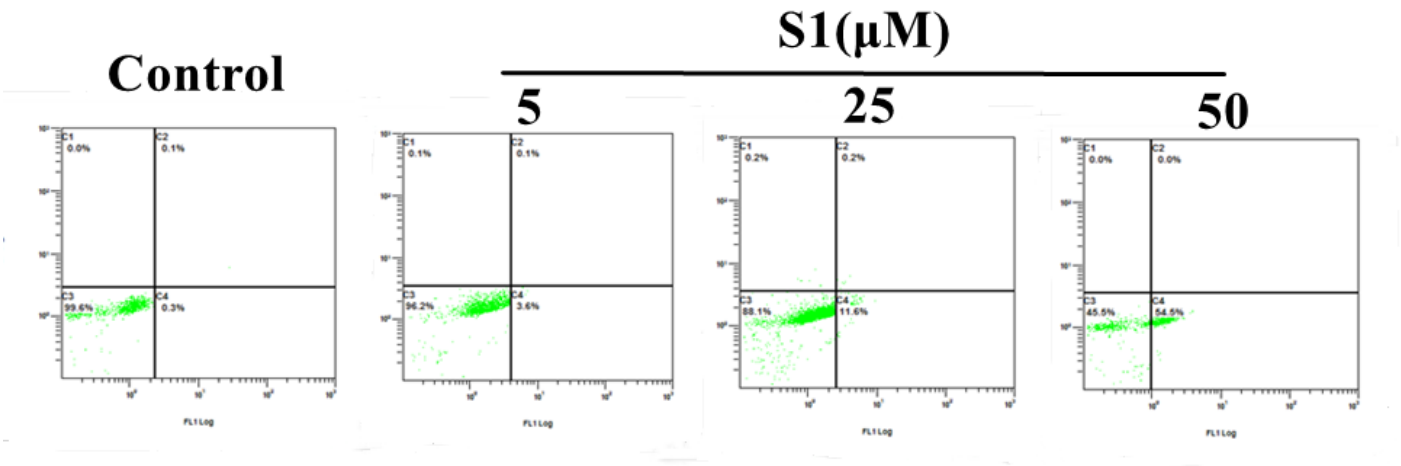

Figure 12

The percentage of living (B3), late apoptotic (B1), and early apoptotic (B4) C33A cells

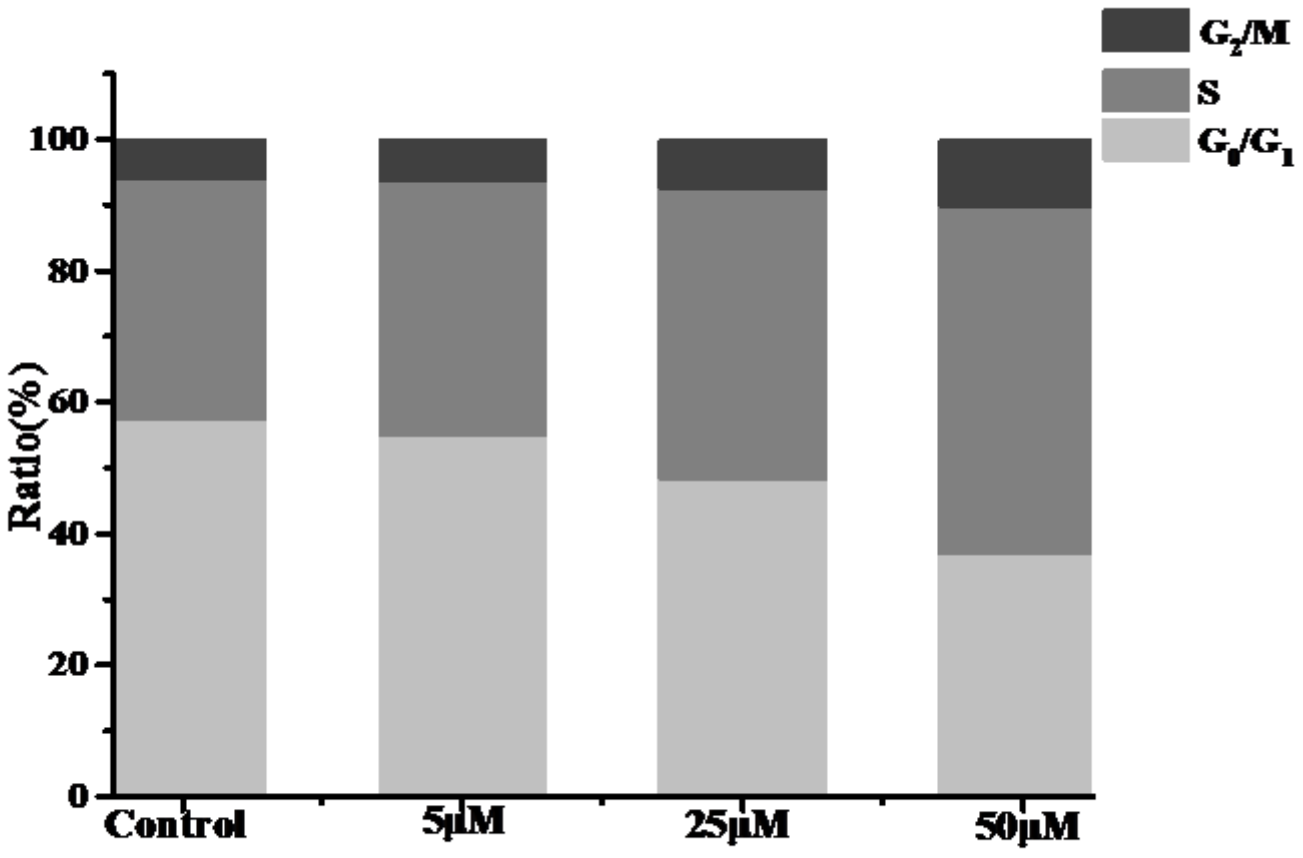

Figure 13

Cell cycle distribution on exposure of C33A cells to 5、25、50 μM S1 complex